On transport in edge islands

Gianluca Spizzo, Matteo Agostini, Paolo Scarin
Nicola Vianello, Roscoe White[1], Oliver Schmitz[2], Monica Spolaore
David Terranova, and Marco Veranda

Consorzio RFX and CNR Padova, Italy
[1] PPPL, Princeton, NJ
[2] Department of Engineering Physics, UoW Madison, WI

643rd Wilhelm und Else Heraeus Seminar
May 19, 2017

Outline

1. Magnetic islands are spontaneously present in the reversed-field pinch (RFP) and stellarator edge, and produced via MP in tokamaks

Outline

1. Magnetic islands are spontaneously present in the reversed-field pinch (RFP) and stellarator edge, and produced via MP in tokamaks
2. Magnetic islands in the edge plasma cause a differential radial diffusion of electrons and ions;

Outline

1. Magnetic islands are spontaneously present in the reversed-field pinch (RFP) and stellarator edge, and produced via MP in tokamaks
2. Magnetic islands in the edge plasma cause a differential radial diffusion of electrons and ions;
3. This results in a strong, positive radial electric field $E^r > 0$ pointing outward the island O-point

Outline

1. Magnetic islands are spontaneously present in the reversed-field pinch (RFP) and stellarator edge, and produced via MP in tokamaks
2. Magnetic islands in the edge plasma cause a differential radial diffusion of electrons and ions;
3. This results in a strong, positive radial electric field $E^r > 0$ pointing outward the island O-point
4. Measurements confirm that kinetic properties of the plasma edge are modulated by edge-resonant islands (induced or spontaneous): in particular, electric fields and associated $\vec{E} \times \vec{B}$ flows follow the symmetry of the dominant mode

Outline

1. Magnetic islands are spontaneously present in the reversed-field pinch (RFP) and stellarator edge, and produced via MP in tokamaks
2. Magnetic islands in the edge plasma cause a differential radial diffusion of electrons and ions;
3. This results in a strong, positive radial electric field $E^r > 0$ pointing outward the island O-point
4. Measurements confirm that kinetic properties of the plasma edge are modulated by edge-resonant islands (induced or spontaneous): in particular, electric fields and associated $\vec{E} \times \vec{B}$ flows follow the symmetry of the dominant mode
5. The $\vec{E} \times \vec{B}$ flows form *convective cells* around the island. These cells, in some conditions, can dominate particle transport in the edge, as in the case of the RFP at high density [Puiatti 2009]

Outline

1. Magnetic islands are spontaneously present in the reversed-field pinch (RFP) and stellarator edge, and produced via MP in tokamaks
2. Magnetic islands in the edge plasma cause a differential radial diffusion of electrons and ions;
3. This results in a strong, positive radial electric field $E^r > 0$ pointing outward the island O-point
4. Measurements confirm that kinetic properties of the plasma edge are modulated by edge-resonant islands (induced or spontaneous): in particular, electric fields and associated $\vec{E} \times \vec{B}$ flows follow the symmetry of the dominant mode
5. The $\vec{E} \times \vec{B}$ flows form *convective cells* around the island. These cells, in some conditions, can dominate particle transport in the edge, as in the case of the RFP at high density [Puiatti 2009]

Outline II

1. What is the origin of these $\vec{E} \times \vec{B}$ flows?

Outline II

1. What is the origin of these $\vec{E} \times \vec{B}$ flows?
2. An analytic form of potential has been introduced in test-particle simulations with ORBIT to satisfy the ambipolarity condition $\Gamma_e = \Gamma_i$, and compared with data in the RFX-mod reversed-field pinch and the TEXTOR Tokamak [Ciaccio 2015];

Outline II

1. What is the origin of these $\vec{E} \times \vec{B}$ flows?
2. An analytic form of potential has been introduced in test-particle simulations with ORBIT to satisfy the ambipolarity condition $\Gamma_e = \Gamma_i$, and compared with data in the RFX-mod reversed-field pinch and the TEXTOR Tokamak [Ciaccio 2015];
3. the potential has the form $\Phi(r, \theta, \zeta) = \Phi_0(r) \sin u$, with $u = m\theta - n\zeta$ the helical angle

Outline II

1. What is the origin of these $\vec{E} \times \vec{B}$ flows?
2. An analytic form of potential has been introduced in test-particle simulations with ORBIT to satisfy the ambipolarity condition $\Gamma_e = \Gamma_i$, and compared with data in the RFX-mod reversed-field pinch and the TEXTOR Tokamak [Ciaccio 2015];
3. the potential has the form $\Phi(r, \theta, \zeta) = \Phi_0(r) \sin u$, with $u = m\theta - n\zeta$ the helical angle
4. Two solutions are possible, which resemble the ion- and electron-roots in stellarators: possibility of interacting with this potential with local heating (ECRH/ICRH);

Outline II

1. What is the origin of these $\vec{E} \times \vec{B}$ flows?
2. An analytic form of potential has been introduced in test-particle simulations with ORBIT to satisfy the ambipolarity condition $\Gamma_e = \Gamma_i$, and compared with data in the RFX-mod reversed-field pinch and the TEXTOR Tokamak [Ciaccio 2015];
3. the potential has the form $\Phi(r, \theta, \zeta) = \Phi_0(r) \sin u$, with $u = m\theta - n\zeta$ the helical angle
4. Two solutions are possible, which resemble the ion- and electron-roots in stellarators: possibility of interacting with this potential with local heating (ECRH/ICRH);
5. Recent results show that this electrostatic response has symmetry m/n only as a first approximation, higher harmonics $(m \pm k)/n$, $k = 1, 2 \ldots$ toroidally couple to the base mode [Agostini 2016]

Outline II

1. What is the origin of these $\vec{E} \times \vec{B}$ flows?
2. An analytic form of potential has been introduced in test-particle simulations with ORBIT to satisfy the ambipolarity condition $\Gamma_e = \Gamma_i$, and compared with data in the RFX-mod reversed-field pinch and the TEXTOR Tokamak [Ciaccio 2015];
3. the potential has the form $\Phi(r, \theta, \zeta) = \Phi_0(r) \sin u$, with $u = m\theta - n\zeta$ the helical angle
4. Two solutions are possible, which resemble the ion- and electron-roots in stellarators: possibility of interacting with this potential with local heating (ECRH/ICRH);
5. Recent results show that this electrostatic response has symmetry m/n only as a first approximation, higher harmonics $(m \pm k)/n$, $k = 1, 2 \ldots$ toroidally couple to the base mode [Agostini 2016]
6. This is illustrated with the method of the Poincaré Recurrence Time, applied for the first time to plasma physics

Outline II

1. What is the origin of these $\vec{E} \times \vec{B}$ flows?
2. An analytic form of potential has been introduced in test-particle simulations with ORBIT to satisfy the ambipolarity condition $\Gamma_e = \Gamma_i$, and compared with data in the RFX-mod reversed-field pinch and the TEXTOR Tokamak [Ciaccio 2015];
3. the potential has the form $\Phi(r, \theta, \zeta) = \Phi_0(r) \sin u$, with $u = m\theta - n\zeta$ the helical angle
4. Two solutions are possible, which resemble the ion- and electron-roots in stellarators: possibility of interacting with this potential with local heating (ECRH/ICRH);
5. Recent results show that this electrostatic response has symmetry m/n only as a first approximation, higher harmonics $(m \pm k)/n$, $k = 1, 2 \ldots$ toroidally couple to the base mode [Agostini 2016]
6. This is illustrated with the method of the Poincaré Recurrence Time, applied for the first time to plasma physics

Measurements of convective cells around islands

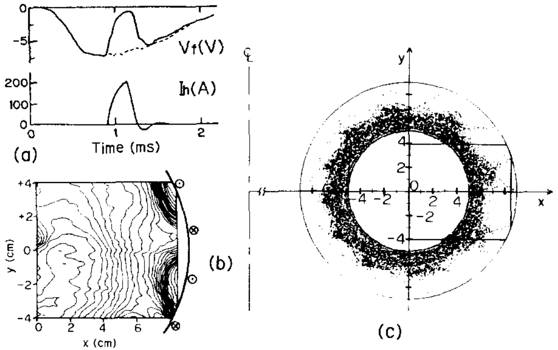

- Example from [Takamura 1987]: measurements of floating potential V_f during application of RMP (a), poloidal map of V_f (b), and comparison with a Poincaré plot (c);
- In TEXT simple diffusion was not capable of describing density profiles during RMP application: strong convective flux was necessary [Evans 1987].

RMP at TEXTOR

TEXTOR was a (much beloved) circular tokamak with limiter in Jülich, Germany (shut down in December 2013). It was capable of producing a stochastic edge via the "Dynamic Ergodic Divertor" (DED), with main resonance at the $q = 3$ surface [Schmitz 2008]

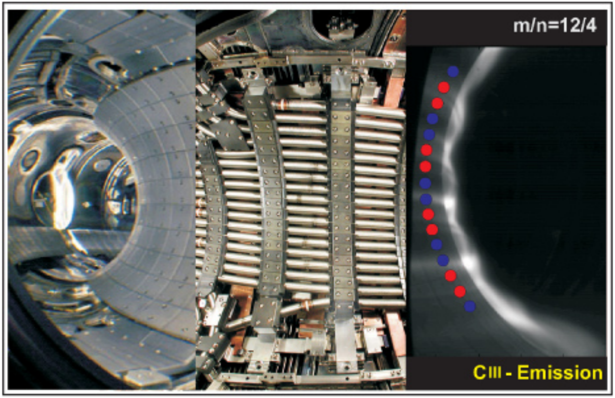

Ripple of E^r in TEXTOR

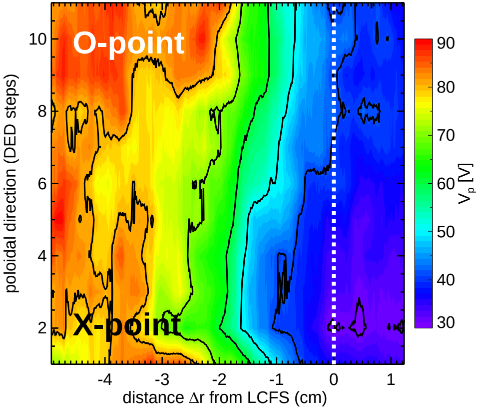

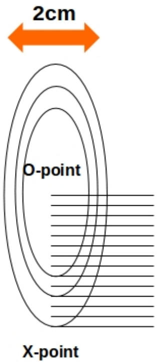

- Measurements of plasma potential inside a $m/n = 4/1$ island;
- Excess of V_p towards the island O-point (OP) and decrease (potential well) towards the X-point (XP) [Ciaccio 2015]

Test-particle simulations with ORBIT

- We use the guiding-center code ORBIT [White 1984] to analyze the magnetic field topology and the motion of monoenergetic electrons and ions embedded in the magnetic field
- ORBIT is in Boozer co-ordinates (ψ_p, θ, ζ)
- TEXTOR: input=analytic form for the radial (resonant) perturbation induced by the DED, based on current levels in the coils [Abdullaev 2014]
- Collisions are implemented as pitch-angle and energy scattering between particles, using the Boozer-Kuo approach [Boozer 1981]
- particles are monoenergetic

Topology of stochastic edge in TEXTOR

Poincaré plot with RMP

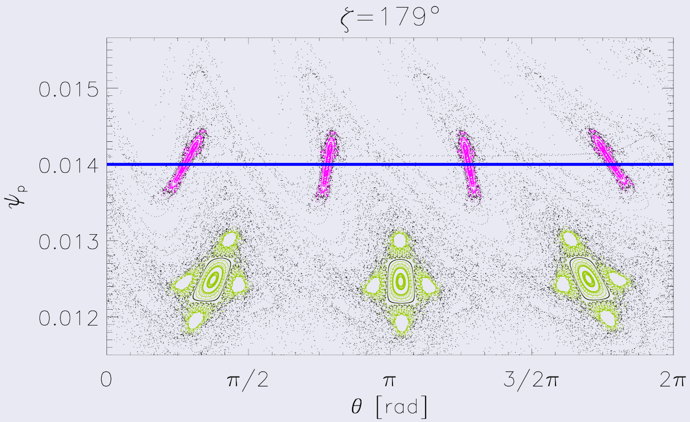

"Base mode" is the 3/1, while the "secondary islands" are 4/1 resonating at $q = 4$ (horizontal line) [Schmitz 2008]

Simulations - Parallel connection lengths - TEXTOR

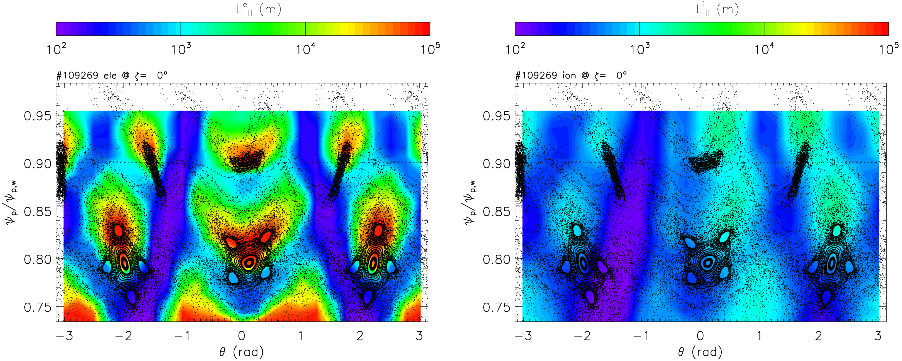

- LEFT=electrons, RIGHT=ions $\longrightarrow$ ion $L^i_{||}$ more uniform along θ
- **ions =larger drifts**
- $L^e_{||}$ has the same symmetry as the RMP helicity (4/1 in this case)

Simulations - D_e, D_i (TEXTOR with RMP)

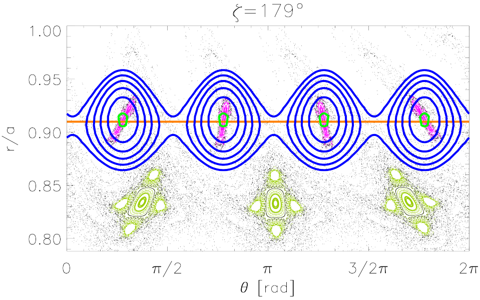

- **Evaluate steady state distributions** $n(\psi)$ by fixing source and sink [Spizzo&White 2009]
- Choose small (helical) domain, reinsert lost particles at the center with uniform pitch
- Find D from flux of particles leaving the domain and the density gradient

Simulations - D_e, D_i (TEXTOR with RMP)

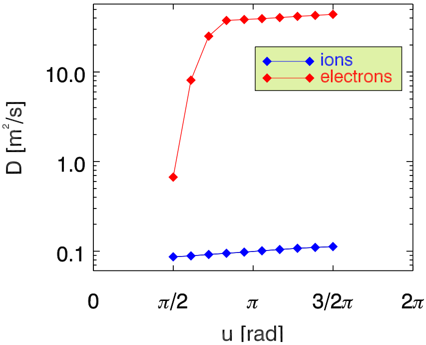

- **Evaluate steady state distributions** $n(\psi)$ by fixing source and sink [Spizzo&White 2009]
- Choose small (helical) domain, reinsert lost particles at the center with uniform pitch
- Find D from flux of particles leaving the domain and the density gradient

- D_i almost neoclassical, small change along u; $D_e \gg D_i$ everywhere
- $D_e \gg D_i$ at the XP, $D_e \approx D_i$ at the OP $\rightarrow E^r \sim 0$ at the OP [Ida 2001]

Model of ambipolar potential

- Up to now, electrons and ions are evolved indipendently one to the other
- Require ambipolarity: $\Gamma_e = \Gamma_i$ at some flux surface (e.g., the LCFS)
- Insert a model of potential $\Phi(\psi_p, \theta, \zeta)$ into ORBIT guiding-center equations

$$\Phi(\psi_p, \theta, \zeta) = \Phi_0 \left[f_1(\psi_p) + \frac{1}{2}(f_2(\psi_p) - f_1(\psi_p)) \sin(-m\theta + n\zeta + \tilde{\phi}) \right], \tag{1}$$

- angular dependence $\rightarrow$ the helical angle
- radial dependence is not simply *const*. $\times\ \psi_p$, but contains the radial functions f_1, f_2 which are deduced from the experiment (it is the only ansatz in the model)
- free parameters = amplitude Φ_0 and phase $\tilde{\phi}$

Map of plasma potential: measurements, model

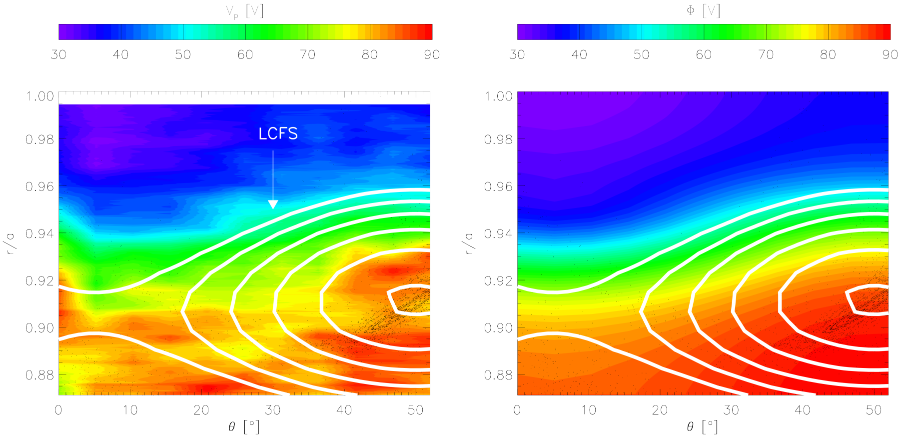

- LEFT=measurements, remapped on helical flux surfaces
- RIGHT= model, phase $\tilde{\phi} = const.$ (fixed RMP)

Ambipolar roots w/ RMP

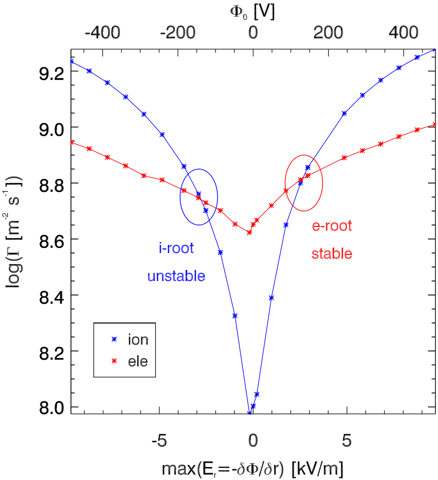

- It is possible to vary the amplitude Φ_0 and check the ambipolar solution $\Gamma_e = \Gamma_i$
- Same tool used in the stellarator community to determine the electron- and ion-roots [Hastings 1985]
- With RMPs, both ion- and electron-dominated transport regimes can exist [Ciaccio 2015]
- With the experimental T_e and T_i the analogous "electron" root is favored

Radial electric field in TEXTOR

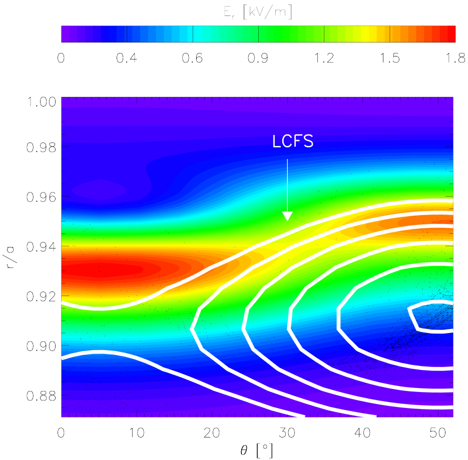

Consequence: strong radial electric field $E^r > 0$ (well known in RMP measurements). As anticipated, $E^r \approx 0$ in the OP, $E^r \gg 0$ in the XP Modulation of E^r along the helical angle u (*convective cell*)

Ambipolar roots w/ RMP

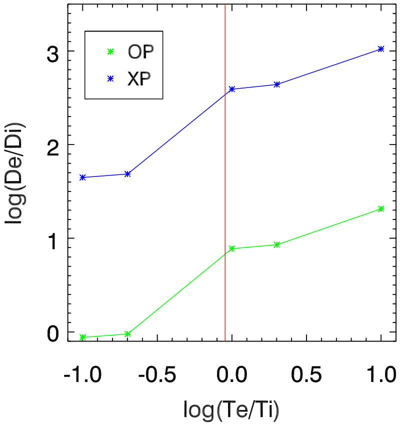

- In stellarators, it is possible to jump from the ion- to the electron-root by using ECRH [Hastings 1985]
- Is it feasible in a tokamak with RMP?
- Sensitivity scan: in the OP the system flips to the ion root ($D_e/D_i < 1$) for $T_e/T_i \lesssim 0.5$

RFX reversed-field pinch (RFP)

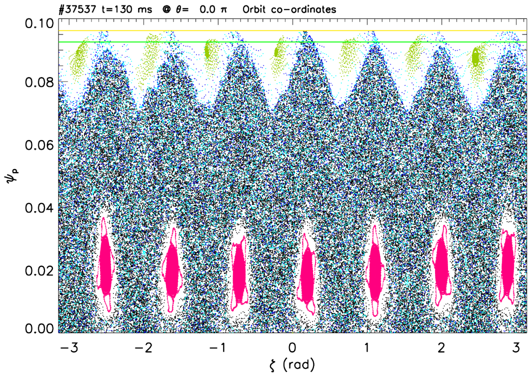

- Poincaré plots, equatorial cut at $\theta = 0$
- input → we solve the Newcomb's equations for tearing modes, toroidal geometry [Zanca 2004]
- Core 1/7 island and edge 0/7 islands resonating at $q = 0$
- Floating potential follows the $n = 7$ periodicity along ϕ [Vianello 2015]

RFX reversed-field pinch (RFP)

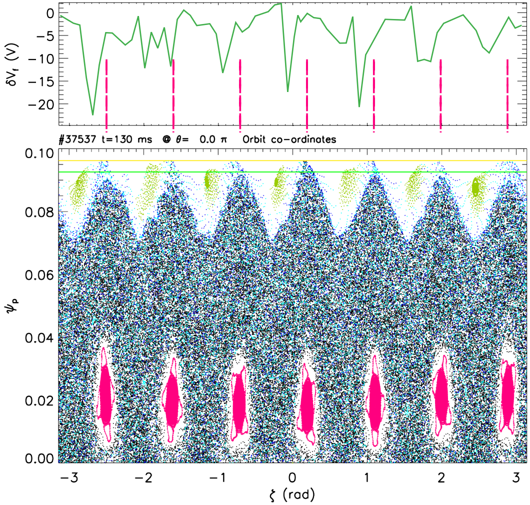

- Poincaré plots, equatorial cut at $\theta = 0$
- input $\rightarrow$ we solve the Newcomb's equations for tearing modes, toroidal geometry [Zanca 2004]
- Core 1/7 island and edge 0/7 islands resonating at $q = 0$
- Floating potential follows the $n = 7$ periodicity along ϕ [Vianello 2015]

Measurements on the same *poloidal* plane

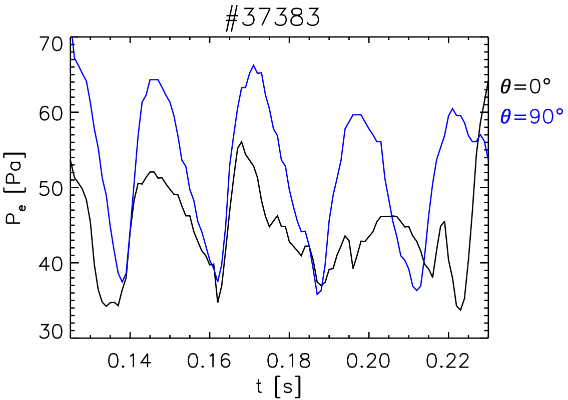

Harmonic hypothesis, $F_k \sim \sin u$, with $u(\theta, \phi; t) = m\theta - n\phi + \omega t$
Measurements in the same poloidal section should follow $F_k = m\theta - \omega t$
$\rightarrow$ with $m = 1$ this means that they should be out-of-phase of $\Delta\theta$
This is not the case, e.g. for electron pressure [Agostini 2016].

Topology: more complicated than a simple helix!

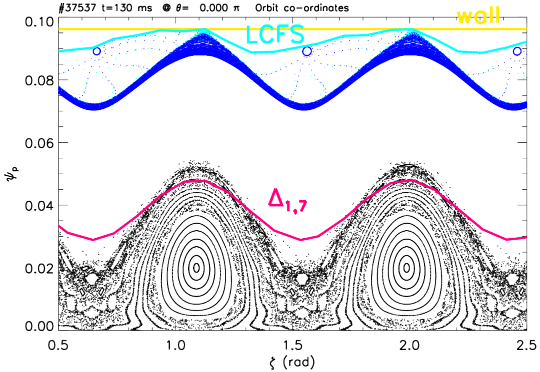

- Poincaré plots, simplified spectrum with $n = 7$ modes, only
- Two structures are visible in the edge: the stochastic layer between the 1/7 and 0/7 resonances
- ...and the orbits around the O-points (OP) of the 0/7 islands

- PWI is determined by the structure closer to the wall [Scarin 2017]

Topology: more complicated than a simple helix!

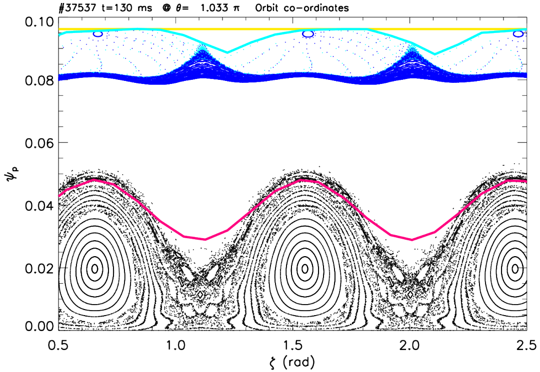

- Poincaré plots, simplified spectrum with $n = 7$ modes, only
- Two structures are visible in the edge: the stochastic layer between the 1/7 and 0/7 resonances
- . . . and the orbits around the O-points (OP) of the 0/7 islands

- PWI is determined by the structure closer to the wall [Scarin 2017]

Full 3D behaviour of (field line) connection lengths

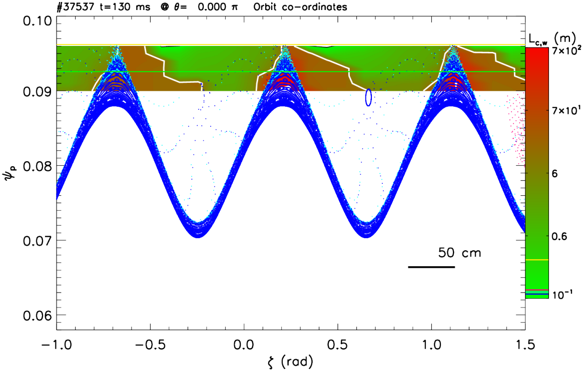

$\theta = \mathbf{0}$

- Calculate the (field line) connection length $L_{c,w}$ to the wall
- It is necessary to analyze the full 3D behaviour
- White contour = value of L_k
- Ergodic regions with $L_{c,w} > L_k$ correspond to minima of V_f [Schmitz 2009]

Full 3D behaviour of (field line) connection lengths

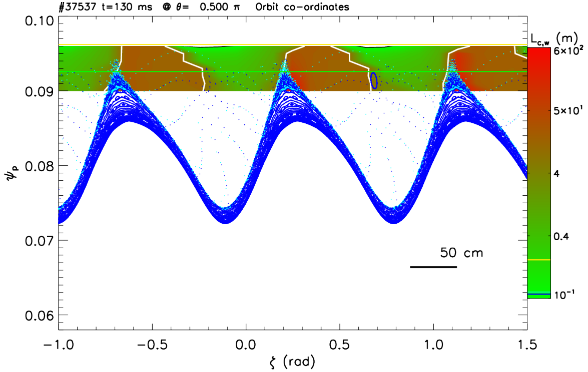

$\theta = \mathbf{90}^{\circ}$

- Calculate the (field line) connection length $L_{c,w}$ to the wall
- It is necessary to analyze the full 3D behaviour
- White contour = value of L_k
- Ergodic regions with $L_{c,w} > L_k$ correspond to minima of V_f [Schmitz 2009]

Full 3D behaviour of (field line) connection lengths

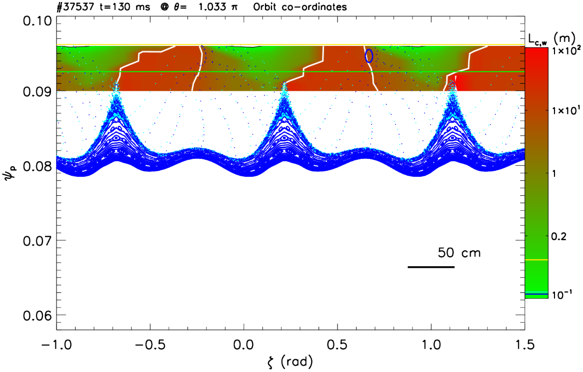

$\theta = 186^\circ$

- Calculate the (field line) connection length $L_{c,w}$ to the wall
- It is necessary to analyze the full 3D behaviour
- White contour = value of L_k
- Ergodic regions with $L_{c,w} > L_k$ correspond to minima of V_f [Schmitz 2009]

Full 3D behaviour of (field line) connection lengths

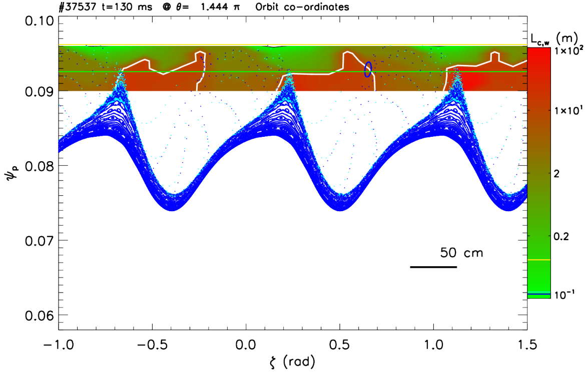

$\theta = 260°$

- Calculate the (field line) connection length $L_{c,w}$ to the wall
- It is necessary to analyze the full 3D behaviour
- White contour = value of L_k
- Ergodic regions with $L_{c,w} > L_k$ correspond to minima of V_f [Schmitz 2009]

$L_{c,w}$ on the (θ, ϕ) plane

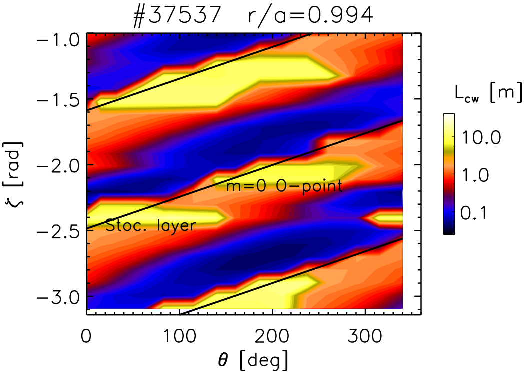

- Another way of seeing this result: $L_{c,w}$ on the (θ, ϕ) plane
- Solid lines = location of the OP of the 1/7 island
- PWI has a strong non-helical component due to the 0/7 mode [Agostini 2017]

Poincaré Recurrence Time

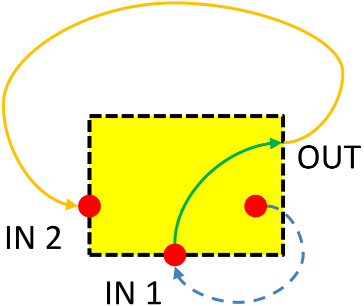

- Problem with connection length: ill-defined metric, it depends on starting and endpoints
- Good metric: Poincaré Recurrence Time = intrinsic property of a volume in phase-space if dynamics are area-preserving [Zaslavsky 2004]

Poincaré Recurrence Time

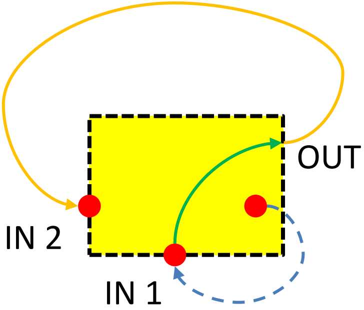

- Problem with connection length: ill-defined metric, it depends on starting and endpoints
- Good metric: Poincaré Recurrence Time = intrinsic property of a volume in phase-space if dynamics are area-preserving [Zaslavsky 2004]
- Define an area A: the **escape time** is

$$\tau^{(\mathrm{esc})} = t_{OUT} - t_{IN1} \qquad (2)$$

Poincaré Recurrence Time

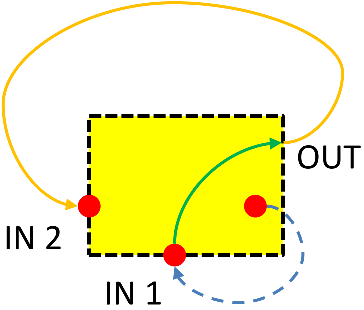

- Problem with connection length: ill-defined metric, it depends on starting and endpoints
- Good metric: Poincaré Recurrence Time = intrinsic property of a volume in phase-space if dynamics are area-preserving [Zaslavsky 2004]
- Define an area A: the **escape time** is

$$\tau^{(\mathrm{esc})} = t_{OUT} - t_{IN1} \qquad (2)$$

- **Time outside** A is

$$\tau^{(\mathrm{ext})} = t_{IN2} - t_{OUT} \qquad (3)$$

Poincaré Recurrence Time

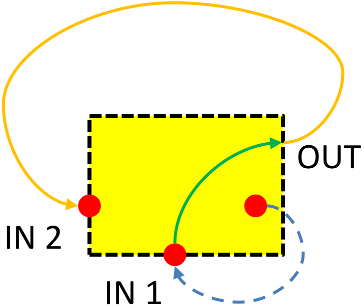

- Problem with connection length: ill-defined metric, it depends on starting and endpoints
- Good metric: Poincaré Recurrence Time = intrinsic property of a volume in phase-space if dynamics are area-preserving [Zaslavsky 2004]
- Define an area A: the **escape time** is

$$\tau^{(\mathrm{esc})} = t_{OUT} - t_{IN1} \qquad (2)$$

- **Time outside** A is

$$\tau^{(\mathrm{ext})} = t_{IN2} - t_{OUT} \qquad (3)$$

- The *recurrence time* is

$$\boxed{\tau^{(\mathrm{rec})} = \tau^{(\mathrm{esc})} + \tau^{(\mathrm{ext})} = t_{IN2} - t_{IN1}} \qquad (4)$$

P.d.f. of recurrences

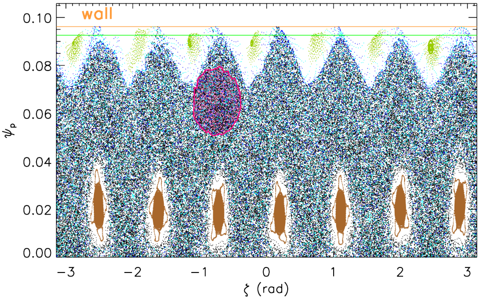

- Start with a fairly large domain A, within the stochastic layer

P.d.f. of recurrences

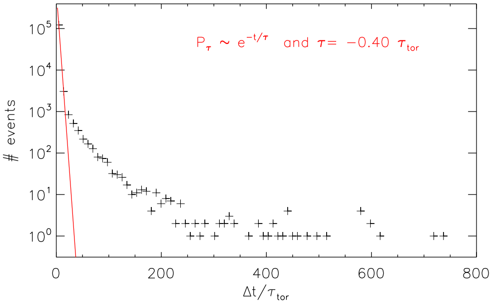

- Start with a fairly large domain A, within the stochastic layer
- p.d.f shows an initial exponential decay $\sim e^{-t/\tau_{\rm mix}}$ being $\tau_{\rm mix} = v_{th} L_k$

P.d.f. of recurrences

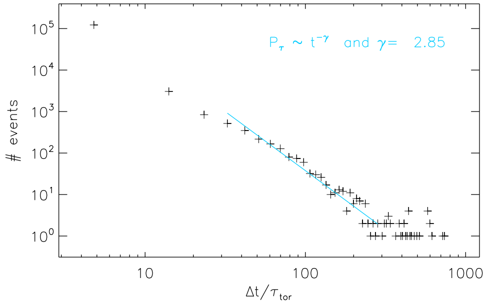

- Start with a fairly large domain A, within the stochastic layer
- p.d.f shows an initial exponential decay $\sim e^{-t/\tau_{\rm mix}}$ being $\tau_{\rm mix} = v_{th} L_k$
- ...then an algebraic tail $\sim t^{-\gamma}$, $\gamma \sim 3$

P.d.f. of recurrences

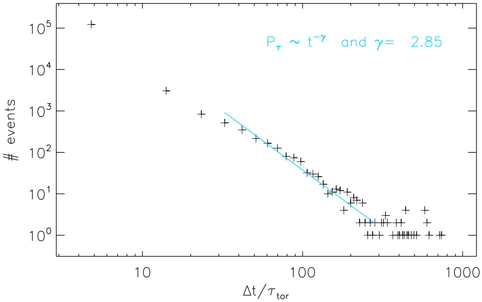

- Start with a fairly large domain A, within the stochastic layer
- p.d.f shows an initial exponential decay $\sim e^{-t/\tau_{\rm mix}}$ being $\tau_{\rm mix} = v_{th} L_k$
- ...then an algebraic tail $\sim t^{-\gamma}$, $\gamma \sim 3$

- The average recurrence time

$$\tau_{\rm rec} = \frac{\int_0^{+\infty} t\, P(t) {\rm d}t}{\int_0^{+\infty} P(t) {\rm d}t} \qquad (5)$$

gives info on the "stickiness" of A

Application of the method to edge islands

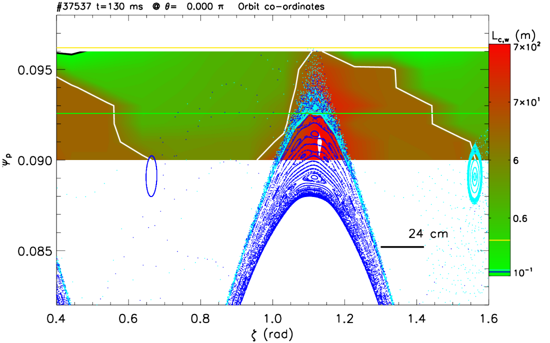

- Let us go back to the contour plot of $L_{c,w}$ at $\theta = 0$.

Application of the method to edge islands

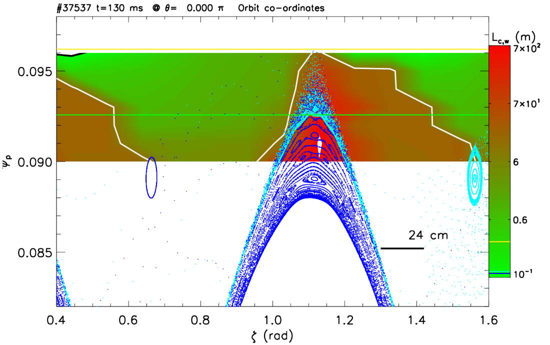

- Let us go back to the contour plot of $L_{c,w}$ at $\theta = 0$.
- Define a 12×6 array of volumes in the (ϕ, r) plane, to calculate Poincaré recurrences

Application of the method to edge islands

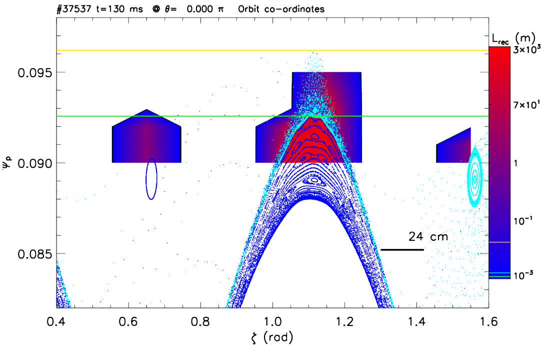

- Let us go back to the contour plot of $L_{c,w}$ at $\theta = 0$.
- Define a 12×6 array of volumes in the (ϕ, r) plane, to calculate Poincaré recurrences
- The ergodic region is the stochastic layer, and corresponds to larger recurrence times

Application of the method to edge islands

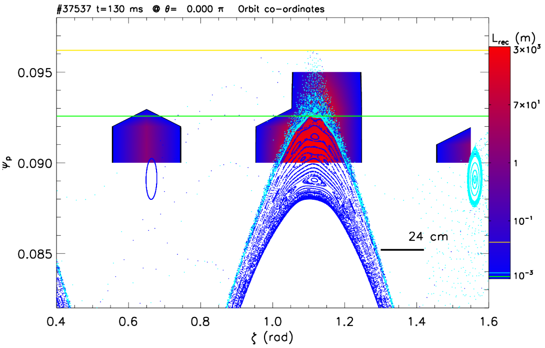

- Let us go back to the contour plot of $L_{c,w}$ at $\theta = 0$.
- Define a 12×6 array of volumes in the (ϕ, r) plane, to calculate Poincaré recurrences
- The ergodic region is the stochastic layer, and corresponds to larger recurrence times
- No recurrences in laminar regions with $L_{c,w} < L_k$

Application of the method to edge islands

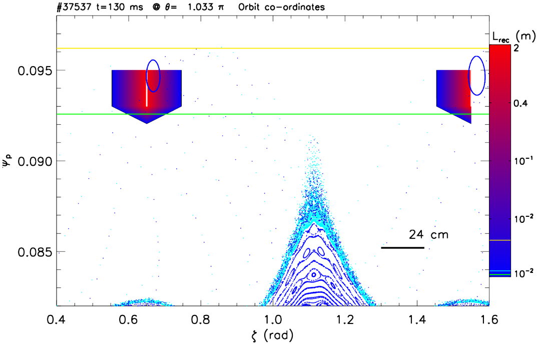

- Let us go back to the contour plot of $L_{c,w}$ at $\theta = 0$.
- Define a 12×6 array of volumes in the (ϕ, r) plane, to calculate Poincaré recurrences
- The ergodic region is the stochastic layer, and corresponds to larger recurrence times
- No recurrences in laminar regions with $L_{c,w} < L_k$

- At $\theta = 186°$ larger recurrence times are near the OP's of the 0/7 islands, as shown in slide # 19

Conclusions

- Magnetic islands in the edge plasma generate an ambipolar potential with their symmetry, as deduced from measurements of E^r and flow

Conclusions

- Magnetic islands in the edge plasma generate an ambipolar potential with their symmetry, as deduced from measurements of E^r and flow
- Test particle simulations in TEXTOR with the 4/1 RMP, can reliably reproduce a modulation of the parallel connection length $L_{\|}$ with the same symmetry as the parent island, and an electrostatic potential with symmetry $\Phi(r, \theta, \zeta) = \Phi_0(r) \sin u$, being $u = m\theta - n\zeta$ the helical angle.

Conclusions

- Magnetic islands in the edge plasma generate an ambipolar potential with their symmetry, as deduced from measurements of E^r and flow
- Test particle simulations in TEXTOR with the 4/1 RMP, can reliably reproduce a modulation of the parallel connection length $L_{\|}$ with the same symmetry as the parent island, and an electrostatic potential with symmetry $\Phi(r, \theta, \zeta) = \Phi_0(r) \sin u$, being $u = m\theta - n\zeta$ the helical angle.
- The dependence on both r and u (helical angle) is consistent with the presence of a *convective cell*, which dominates transport especially at high density [Spizzo 2010].

Conclusions

- Magnetic islands in the edge plasma generate an ambipolar potential with their symmetry, as deduced from measurements of E^r and flow
- Test particle simulations in TEXTOR with the 4/1 RMP, can reliably reproduce a modulation of the parallel connection length $L_{||}$ with the same symmetry as the parent island, and an electrostatic potential with symmetry $\Phi(r, \theta, \zeta) = \Phi_0(r) \sin u$, being $u = m\theta - n\zeta$ the helical angle.
- The dependence on both r and u (helical angle) is consistent with the presence of a *convective cell*, which dominates transport especially at high density [Spizzo 2010].
- Further studies in RFX-mod reversed-field pinch show that the helical assumption $\Phi \sim \Phi_0(r) \sin u$ is valid only at order zero.

Conclusions

- Magnetic islands in the edge plasma generate an ambipolar potential with their symmetry, as deduced from measurements of E^r and flow
- Test particle simulations in TEXTOR with the 4/1 RMP, can reliably reproduce a modulation of the parallel connection length $L_{\parallel}$ with the same symmetry as the parent island, and an electrostatic potential with symmetry $\Phi(r, \theta, \zeta) = \Phi_0(r) \sin u$, being $u = m\theta - n\zeta$ the helical angle.
- The dependence on both r and u (helical angle) is consistent with the presence of a *convective cell*, which dominates transport especially at high density [Spizzo 2010].
- Further studies in RFX-mod reversed-field pinch show that the helical assumption $\Phi \sim \Phi_0(r) \sin u$ is valid only at order zero.
- Higher harmonics toroidally coupled to the base mode 1/7 are important in determining the complete 3D electrostatic response, and associated plasma-wall interaction.

Conclusions

- Magnetic islands in the edge plasma generate an ambipolar potential with their symmetry, as deduced from measurements of E^r and flow
- Test particle simulations in TEXTOR with the 4/1 RMP, can reliably reproduce a modulation of the parallel connection length $L_{\|}$ with the same symmetry as the parent island, and an electrostatic potential with symmetry $\Phi(r,\theta,\zeta) = \Phi_0(r)\sin u$, being $u = m\theta - n\zeta$ the helical angle.
- The dependence on both r and u (helical angle) is consistent with the presence of a *convective cell*, which dominates transport especially at high density [Spizzo 2010].
- Further studies in RFX-mod reversed-field pinch show that the helical assumption $\Phi \sim \Phi_0(r)\sin u$ is valid only at order zero.
- Higher harmonics toroidally coupled to the base mode 1/7 are important in determining the complete 3D electrostatic response, and associated plasma-wall interaction.
- This result is confirmed through the Poincaré Recurrence Time calculation, which is a better defined metric w.r.t. the connection length

Conclusions

- Magnetic islands in the edge plasma generate an ambipolar potential with their symmetry, as deduced from measurements of E^r and flow
- Test particle simulations in TEXTOR with the 4/1 RMP, can reliably reproduce a modulation of the parallel connection length $L_{||}$ with the same symmetry as the parent island, and an electrostatic potential with symmetry $\Phi(r, \theta, \zeta) = \Phi_0(r) \sin u$, being $u = m\theta - n\zeta$ the helical angle.
- The dependence on both r and u (helical angle) is consistent with the presence of a *convective cell*, which dominates transport especially at high density [Spizzo 2010].
- Further studies in RFX-mod reversed-field pinch show that the helical assumption $\Phi \sim \Phi_0(r) \sin u$ is valid only at order zero.
- Higher harmonics toroidally coupled to the base mode 1/7 are important in determining the complete 3D electrostatic response, and associated plasma-wall interaction.
- This result is confirmed through the Poincaré Recurrence Time calculation, which is a better defined metric w.r.t. the connection length

Future plans

- The ambipolar mechanism implies the presence of multiple solutions

Future plans

- The ambipolar mechanism implies the presence of multiple solutions
- In principle, it is possible to "jump" from one solution to the other by acting on T_e/T_i

Future plans

- The ambipolar mechanism implies the presence of multiple solutions
- In principle, it is possible to "jump" from one solution to the other by acting on T_e/T_i
- FTU & ASDEX-U: existing experiments of ECRH targeted on the 2/1 resonance at high β show dramatic effects on transport [Esposito & Granucci 2008]

Future plans

- The ambipolar mechanism implies the presence of multiple solutions
- In principle, it is possible to "jump" from one solution to the other by acting on T_e/T_i
- FTU & ASDEX-U: existing experiments of ECRH targeted on the 2/1 resonance at high β show dramatic effects on transport [Esposito & Granucci 2008]
- This possibility is being explored in AUG within the EUROfusion MST1 Workpackage (High Level Topic #7)

Future plans

- The ambipolar mechanism implies the presence of multiple solutions
- In principle, it is possible to "jump" from one solution to the other by acting on T_e/T_i
- FTU & ASDEX-U: existing experiments of ECRH targeted on the 2/1 resonance at high β show dramatic effects on transport [Esposito & Granucci 2008]
- This possibility is being explored in AUG within the EUROfusion MST1 Workpackage (High Level Topic #7)

References I

- S. Abdullaev 2014 *Magnetic Stochasticity in Magnetically Confined Fusion Plasmas*, Springer Series on Atomic, Optical, and Plasma Physics Vol. 78
- M. Agostini and P. Scarin 2016 *Proc. 26th IAEA Fusion Energy Conference* paper EX-D/310
- M. Agostini, P. Scarin, G. Spizzo *et al.* 2017 *Nucl. Fusion* Accepted paper, in press
- Allen H. Boozer and Gioietta Kuo-Petravic 1981 *Phys. of Fluids* **24** 851–859
- G. Ciaccio, O. Schmitz *et al.* 2015 *Phys. Plasmas* **22** 102516
- B. Esposito, G. Granucci *et al.* 2008 *Phys. Rev. Lett.* **100** 045006
- T. E. Evans *et al.* 1987 *Proc. of the 14$^{\mathrm{th}}$ EPS Conference on Plasma Physics* vol. 11D, pp.770–773.
- D. Hastings, W. Houlberg and K. Shaing 1985 *Nucl. Fusion* **25** 445
- K. Ida *et al.* 2001 *Phys. Rev. Lett.* **88** 015002

References II

- M.E.Puiatti *et al.* 2009 *Phys. Plasmas* **16** 012505
- P.Scarin *et al.* 2017 *Nuclear Materials and Energy* In Press, Corrected Proof
- O. Schmitz *et al.* 2008 *Nucl. Fusion* **48** 024009
- O. Schmitz *et al.* 2009 *J. Nucl. Materials* **390-391** 330
- G.Spizzo and R.B.White 2009 *Plasma Phys. Control. Fusion* **51** 124026
- G. Spizzo *et al.* 2010 *Plasma Phys. Control. Fusion* **52** 095011
- S. Takamura *et al.* 1987 *Phys. Fluids* **30** 144
- N.Vianello *et al.* 2013 *Plasma Phys. Control. Fusion* **57** 014027
- R. B. White and M. S. Chance 1984 *Phys. Fluids* **27** 2455-2467
- P. Zanca and D. Terranova 2004 *Plasma Phys. Control. Fusion* **46** 1115
- G. M. Zaslavsky 2004 *Hamiltonian Chaos and Fractional Dynamics*, Oxford University Press, chap.11, pp. 173–186